

**Climatology, seasonality and trends of oceanic coherent
eddies**

Josué Martínez-Moreno¹, Andrew McC. Hogg¹, and Matthew England²

⁴ Research School of Earth Science and ARC Center of Excellence for Climate Extremes, Australian
⁵ National University, Canberra, Australia

⁶ Climate Change Research Centre (CCRC), UNSW Australia, Sydney NSW, Australia

Key Points:

- ⁸ Kinetic energy of coherent eddies contain around 30% of the surface ocean kinetic
⁹ energy budget.
- ¹⁰ Seasonal cycle of the number of coherent eddies and coherent eddy amplitude re-
¹¹ veal a 3-6 month lag to wind forcing
- ¹² The coherent eddy amplitude has increase at a rate of 3 cm per decade since 1993.

13 Abstract

Ocean eddies influence regional and global climate through mixing and transport of heat and properties. One of the most recognizable and ubiquitous feature of oceanic eddies are vortices with spatial scales of tens to hundreds of kilometers, frequently referred as “mesoscale eddies” or “coherent eddies”. Coherent eddies are known to transport properties across the ocean and to locally affect near-surface wind, cloud properties and rainfall patterns. Although coherent eddies are ubiquitous, yet their climatology, seasonality and long-term temporal evolution remains poorly understood. Thus, we examine the kinetic energy contained by coherent eddies and we present the annual, interannual, and long-term changes of automatically identified coherent eddies from satellite observations and a state of the art numerical simulation from 1993 to 2018. Satellite observations show that around 40% of the kinetic energy contained by ocean eddies corresponds to coherent eddies. Additionally, a strong hemispherical seasonal cycle is observed, on top of a 3–6 months lag between the wind forcing and the response of the coherent eddy field. Furthermore, the seasonality of the number of coherent eddies and their amplitude reveals that the number of coherent eddies responds faster to the forcing (~ 3 months), while the coherent eddy amplitude is lagged by ~ 6 months. There are regions that show a pronounced influence of coherent eddies, notably, the East Indian Ocean, the East Tropical Pacific Ocean, and the South Atlantic Ocean. In these locations, a strong seasonal cycle and interannual variability can be observed in both satellite and numerical models. Although, there is agreement between these products on the seasonality of the number of eddies, the seasonality of the coherent eddy amplitude between these products show some inconsistencies. Long-term trends of the coherent eddy amplitude from satellite observations and the state of the art model show significant increases in the eddy amplitude of $\sim 3\text{cm}$ per decade in large portions of the ocean, while the number of coherent eddies remains constant. Our analysis highlight the relative importance of the coherent eddy fiend in the ocean kinetic energy budget, imply a strong response of the eddy number and eddy amplitude to the surface wind at different time-scales, and showcases for the first time seasonality, and multidecadal trends of the coherent eddy properties.

42 Plain language summary

43 1 Introduction

44 Mesoscale ocean variability with spatial scales of tens to hundreds of kilometers is
 45 comprised of processes such as vortices, waves, and jets (Ferrari & Wunsch, 2009; Fu et
 46 al., 2010). These mesoscale processes are highly energetic, and they play a crucial role
 47 in the transport of heat, salt, momentum, and other tracers through the ocean (Wun-
 48 sch & Ferrari, 2004; Wyrtki et al., 1976; Gill et al., 1974). Possibly, the most recogniz-
 49 able and abundant process observed from satellites is mesoscale vortices. Although mesoscale
 50 vortices are commonly referred to in literature as “mesoscale eddies”, this term is also
 51 often used to describe mesoscale ocean variability (time-varying component of flow), thus,
 52 here we will refer to mesoscale vortices as coherent eddies.

53 Coherent eddies are circular currents and according to their rotational direction,
 54 the sea surface height anomaly within a coherent eddy can have a negative or positive
 55 sea surface height anomaly (cold-core and warm-core coherent eddies, respectively). This
 56 characteristic sea surface height signature of coherent eddies has been utilized to auto-
 57 matically identified and tracked coherent eddies from satellite altimetry (Cui et al., 2020;
 58 Martínez-Moreno et al., 2019; Ashkezari et al., 2016; Faghmous et al., 2015; Chelton et
 59 al., 2007). Automated identification algorithms of coherent eddies have shown their ubiq-
 60 uity in the oceans, with a predominant influence at hotspots of eddy activity such as bound-
 61 ary currents and the Antarctic Circumpolar Current. In these regions, Chelton et al. (2011)
 62 estimated that coherent eddies contribute around 40–50% of the mesoscale kinetic en-
 63 ergy (Chelton et al., 2011) and thus a significant fraction of the total kinetic energy (Fer-
 64 rari & Wunsch, 2009). Although this unique estimate showcases the importance of the
 65 mesoscale coherent eddy field, the energy contained by coherent eddies was estimated
 66 by extracting the geostrophic velocities within the detected coherent eddies, thus it is
 67 possible it may contain energy from other processes. Coherent eddies are not only abun-
 68 dant and may have a large proportion of the surface kinetic energy budget, but they also
 69 are essential in the ocean dynamics as concluded by many previous studies (Patel et al.,
 70 2020; Schubert et al., 2019; Pilo et al., 2015; Frenger et al., 2015, 2013; Beron-Vera et
 71 al., 2013; Siegel et al., 2011; Hogg & Blundell, 2006).

72 There is broad consensus that mesoscale eddy kinetic energy has a pronounced sea-
 73 sonal variability (Uchida et al., 2017; Kang & Curchitser, 2017; Qiu & Chen, 2004; Qiu,
 74 1999), several hypotheses proposed to explain this include: seasonal variations of atmo-

spheric forcing (Sasaki et al., 2014), seasonality of the mixed layer depth (Qiu et al., 2014; Callies et al., 2015), seasonality in the intensity of barotropic instability (Qiu & Chen, 2004), the variability of the baroclinic instability due to the seasonality of the vertical shear (Qiu, 1999), and a seasonal lag of the inverse energy cascade (energy is transported between scales from small to large; Arbic et al., 2013) in combination with the presence of a front in the mixed layer, which can lead to a seasonal cycle of the baroclinic instability (Qiu et al., 2014). All these factors are likely to influence the seasonal cycle of coherent eddies, however, the seasonality of the coherent component of the eddy kinetic energy, as well as the seasonal cycle of the coherent eddy statistics remains unknown.

On one hand, processes such as barotropic and baroclinic instabilities could control the seasonality of coherent eddies in the ocean. On the other hand, recent studies using observations and eddy-permitting climate models suggest several long-term adjustments of the global ocean capable of long-term changes in the coherent eddy field. Such readjustments include a multidecadal increase in the ocean stratification resulted from temperature and salinity changes (Li et al., 2020), a horizontal readjustment of the sea surface temperature gradients (Ruela et al., 2020; Bouali et al., 2017; Cane et al., 1997), and an intensification of the kinetic energy, eddy kinetic energy, and mesoscale eddy kinetic energy over the last 3 decades as a consequence of an increase in wind forcing (Hu et al., 2020; Wunsch, 2020; Martínez-Moreno et al., 2021). These readjustments are directly tight with the generation of coherent eddies, thus they could modify the long-term response of the mesoscale coherent eddy field.

Andy suggested moving the previous paragraph somewhere else, but I don't know where would it fit best, I think it will be confusing to introduce long-term trends before the seasonal cycle. Any suggestion? Perhaps merge both paragraphs? i.e. . . . of the baroclinic instability (Qiu et al., 2014). On one hand, processes such as barotropic and baroclinic instabilities could control the seasonality of coherent eddies in the ocean. On the other hand, recent studies . . . All these seasonal factors and long-term readjustments directly influence the annual and decadal response of the coherent eddy field, however, the seasonality of the coherent component of the eddy kinetic energy, as well as the seasonal cycle and trends of the coherent eddy statistics remain unknown. What do you think?

Here we present a new estimate and climatology of the coherent eddy kinetic energy by reconstructing the coherent eddy signature from satellite observations, the seasonal cycle of the coherent eddy kinetic energy, and seasonal cycle and long-term trends

of the coherent eddy properties over the satellite record. Moreover, we investigate regions where coherent eddies dominate the eddy kinetic energy field. This paper is structured as follows: the data sources and methodology are described in section 2. Then, we present the climatology, energy ratios, and global seasonality of the coherent eddy kinetic energy in subsection 3.1. Subsection 3.2 presents the global climatology and seasonality of coherent eddy properties, followed by the seasonal cycle and coherent eddy property time-series in regions dominated by coherent eddies (subsection 3.3). We then focus our attention on the long-term changes of the coherent eddy properties (section 4). Finally, section 5 summarizes the main results and discusses the implications of this study.

2 Methods

2.1 Data

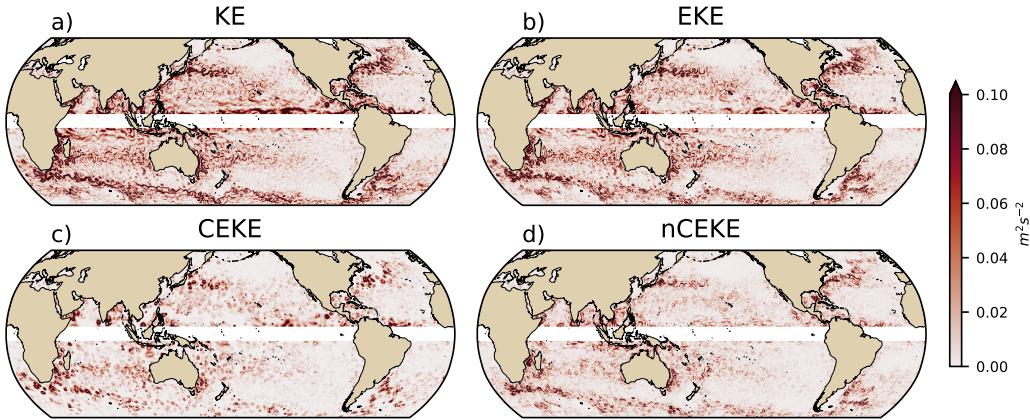
2.2 Coherent eddy identification algorithm

2.3 Kinetic Energy decomposition

Kinetic energy is commonly divided into the mean and time-varying components through a Reynolds decomposition. At a given time, the velocity field $\mathbf{u} = (u, v)$ is split into the time mean ($\bar{\mathbf{u}}$) and time varying components (\mathbf{u}'). Additionally, we further decompose the eddy kinetic energy into the eddy kinetic energy contained by coherent features (\mathbf{u}'_e) and non-coherent (\mathbf{u}'_n). Therefore the KE equation can be written as:

$$\text{KE} = \underbrace{\bar{u}^2 + \bar{v}^2}_{\text{MKE}} + \underbrace{u'_e^2 + v'_e^2}_{\text{CEKE}} + \underbrace{u'_n^2 + v'_n^2}_{\text{nCEKE}} + \mathcal{O}_c^2 + \mathcal{O}^2 \quad (1)$$

Due to the properties of this decomposition, the second order term \mathcal{O}^2 is zero when averaged over the same period as $\bar{\mathbf{u}}$. However, \mathcal{O}_c^2 is only negligible when averaged in time and space. For more information about the decomposition of the field into coherent features and non-coherent features refer to Martínez-Moreno et al. (2019). A global snapshot of each component of kinetic energy decomposition is shown in figure 1, where the imprint of the coherent eddies corresponds to rings of kinetic energy.



131 **Figure 1.** Snapshot of surface kinetic energy (\overline{KE}), surface eddy kinetic energy (\overline{EKE}),
 132 surface coherent eddy kinetic energy (\overline{CEKE}), and surface non-coherent eddy kinetic energy
 133 (\overline{nCEKE}) for the 1st of January 2017.

134 3 Results

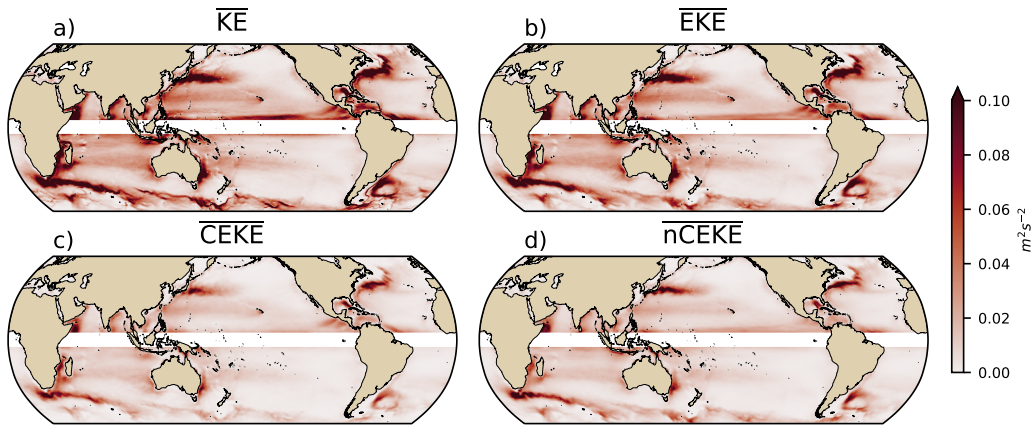
135 3.1 Coherent Eddy Energetics

136 **Figure 2**

- 137 • All KE components have large energy contents in the boundary currents and antarctic
 138 circumpolar current.
- 139 • In many cases is the same, but there actually some differences There are several
 140 regions where the coherent component is larger than the non-coherent, we will in-
 141 vestigate these in more detail in section XX.

145 **Figure 3**

- 146 • \overline{EKE} is responsible of almost all the \overline{KE} across the ocean, except for regions with
 147 persistent currents over time, such as the mean boundary current locations, equatorial
 148 pacific currents and regions in the Antarctic Circumpolar current, where the
 149 EKE explains around 40% of the \overline{KE}
- 150 • This estimate is consistent with that of Chelton.
- 151 • \overline{EKE} Explains 80% of \overline{KE} , while \overline{CEKE} is 45% of \overline{EKE} and \overline{nCEKE} is 60% of
 152 \overline{EKE}
- 153 • \overline{CEKE} is large equatorwards from the Kuroshio current and Agulhas current.



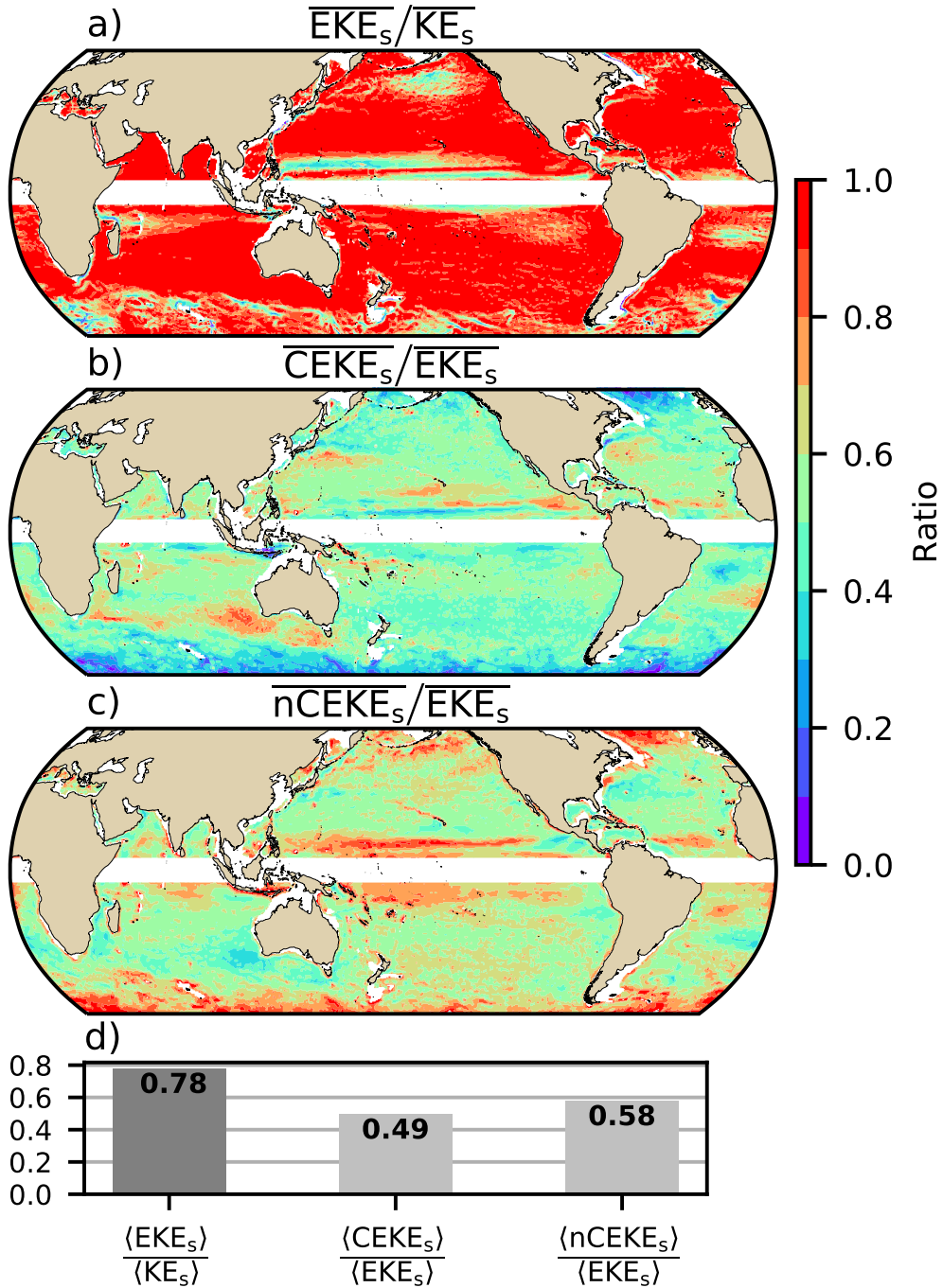
142 **Figure 2.** Climatology of surface kinetic energy (\overline{KE}), surface eddy kinetic energy (\overline{EKE}),
 143 surface coherent eddy kinetic energy (\overline{CEKE}), and surface non-coherent eddy kinetic energy
 144 (\overline{nCEKE}) between 1993-2018.

- 154 • Areas with the largest coherent contribution are located in the South of Australia
 155 \overline{CEKE} and South Atlantic
 156 •
 157 • \overline{nCEKE} has a large amount of energy at high latitudes, this could be a consequence
 158 of the satellites not resolving the mesoscale coherent eddies.
 159 • Global averages of the ratios show \overline{EKE} explains around 78% of the ocean *MKE*
 160 field, while coherent eddies and non coherent eddy features contain 49% and 59%
 161 per decade. Note this values don't add to 1 as there are cross terms that contain
 162 around XX% of the total energy.

171 **3.1.1 Seasonality**

172 **Figure 4**

- 173 • The hemisphere seasonality show the EKE and CEKE peak in summer.
 174 • Response of the EKE and CEKE show a seasonal lag of \sim 6 months to the forcing
 175 of the Winds. Make sure to note the maximum over the hemisphere, locally,
 176 the winds may peak in different months.
 177 • Methods, explain more about winds or here.
 178 • The coherent eddy field show a large interannual variability.



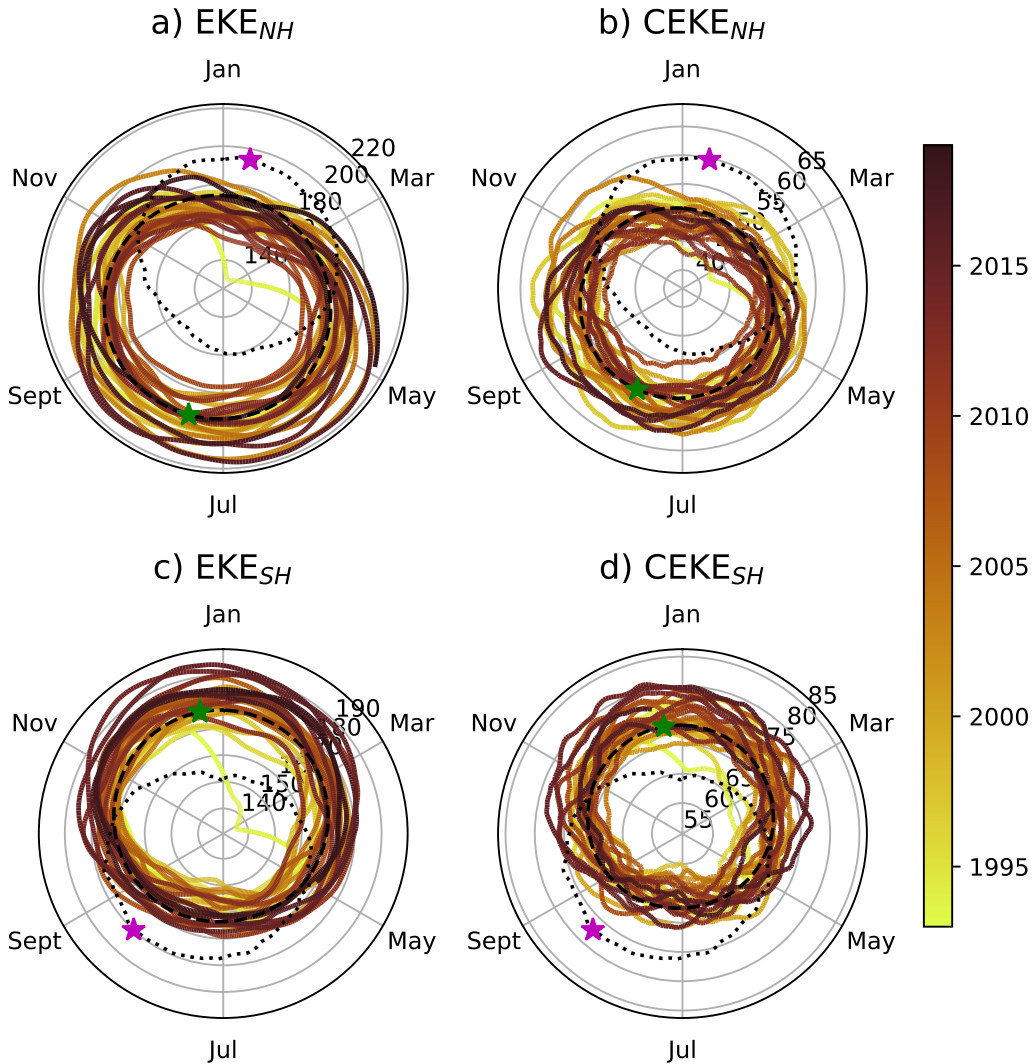
163 **Figure 3.** Ratios of the kinetic energy components. a) Map of the proportion of mean eddy
 164 kinetic energy (EKE_s) versus mean kinetic energy (\overline{KE}); b) Map of the percentage of mean co-
 165 herent eddy kinetic energy (\overline{CEKE}_s) versus mean eddy kinetic energy (\overline{EKE}_s); c) Map of the
 166 percentage of mean non-coherent eddy kinetic energy (\overline{nCEKE}_s) versus mean eddy kinetic energy
 167 (\overline{EKE}_s); d) Global averaged percentage of mean eddy kinetic energy ($\langle \overline{EKE} \rangle$) versus the global
 168 mean kinetic energy ($\langle \overline{KE} \rangle$), and percentage of mean coherent eddy kinetic energy ($\langle \overline{CEKE} \rangle$)
 169 and mean non coherent eddy kinetic energy ($\langle \overline{nCEKE} \rangle$) versus global mean eddy kinetic energy
 170 ($\langle \overline{EKE} \rangle$).

- In the Southern Ocean we observe a concentric growth as time passes, which support the increasing trends in the Southern Ocean observed by (Hogg et al., 2015; Martínez-Moreno et al., 2019, 2021)
- Point that in the northern hemisphere in winter the CEKE appears to be decreasing.

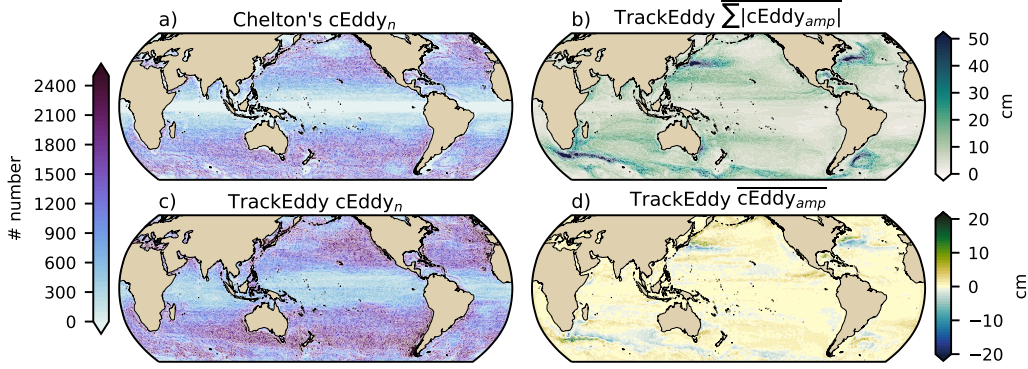
3.2 Coherent Eddy Statistics

Figure 5

- A comparison with previous identified numbers show a consistent pattern in the eddy count. The difference in the magnitude could be a consequence of Chelton et al. (2007) filtering the coherent eddies with lifespans longer than 16 weeks.
- Both datasets show a large number of eddies in the East North Pacific, East North Atlantic, as well as the East South Pacific, East South Atlantic and East Indian Ocean.
- While the number of eddies detected in the tropics is quite small.
- Furthermore, there are hotspots of numbers of eddies in other regions of the ocean, such as boundary currents and the Antarctic Circumpolar Current.
- An interesting feature shown in both datasets is a predominant patchiness where the count of the eddies is much larger. These puzzling pattern remains unknown. Although it looks like a propagation pattern, it could be that eddies persist for longer in those areas.
- The eddy amplitude as expected is maximum at the boundary currents and hotspots in the southern ocean.
- Interior of the gyres we can observe that there is an important amplitude of the coherent eddy field.
- Preferred eddy amplitude sign in boundary currents; positive amplitude polewards to the boundary current mean location, and negative amplitude equatorwards. This is consistent with the shed of coherent eddies from the boundary currents.
- There regions with large CEKE ratio show also a large coherent eddy amplitude.



184 **Figure 4.** Hemispherical seasonality of eddy kinetic energy (EKE), coherent eddy kinetic en-
 185 ergy (CEKE). Panels a, and b show the northern hemisphere seasonal cycle, while panels c, and
 186 d correspond to the southern hemisphere. Dashed lines correspond to the seasonal cycle of the
 187 fields and dotted lines show the seasonal cycle of the wind magnitude smoothed over 120 days
 188 (moving average). The green and magenta stars show the maximum of the seasonal cycle for the
 189 kinetic energy components and the wind magnitude, respectively. The line colors show the year.



213 **Figure 5.** Climatology of the coherent eddy statistics. a) Climatology of the number of coherent
 214 eddies ($cEddy_n$) identified by Chelton et al. (2007); b) Climatology of the warm core coherent
 215 eddy amplitude ($cEddy_{amp}$). c) Climatology of the number of coherent eddies ($cEddy_n$) identified
 216 by Martínez-Moreno et al. (2019); d) Climatology of the cold core coherent eddy amplitude
 217 ($cEddy_{amp}$).

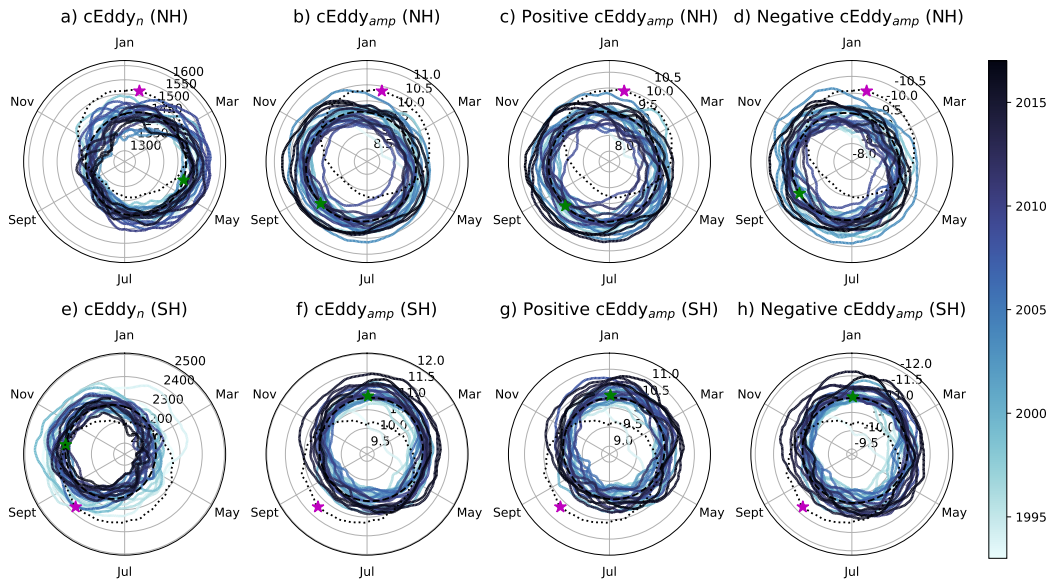
218 3.2.1 Seasonality

219 **Figure 6**

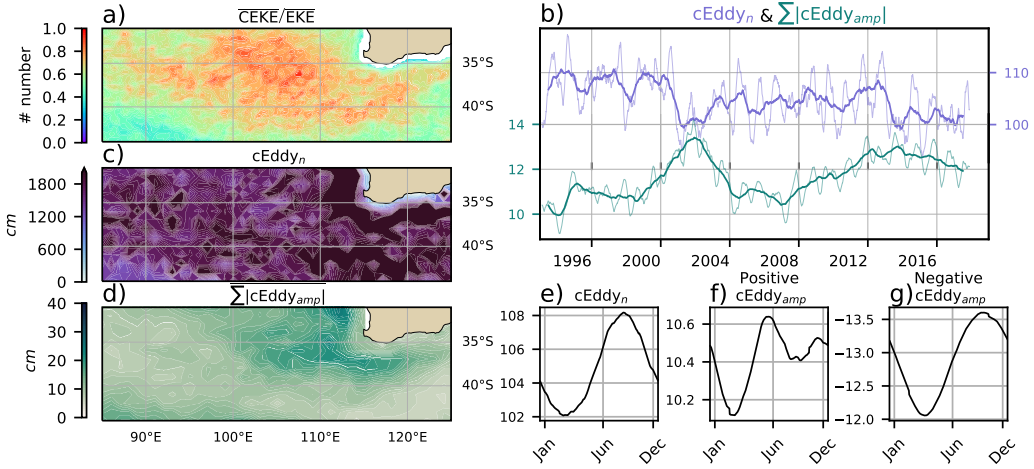
- 220 • Seasonality of the number of eddies in the Northern Hemisphere peaks on May,
 221 while the Southern Hemisphere peaks on October.
- 222 • The seasonality of the amplitude of the eddies is consistent with those of the Co-
 223 herent eddy kinetic energy.
- 224 • Interestingly, there is a 3 month lag between the winds and the seasonality of
 225 the number of eddies, while the eddy amplitude responds approximately 6 months
 226 after the maximum winds.
- 227 • Note that both coherent eddy amplitudes seem to peak around the same time.
- 228 • If we look closely, the growing-shrinking concentric circles correspond to an increasing-
 229 decreasing trend. These are particularly obvious as a decrease in the eddy num-
 230 ber in the Southern Hemisphere, and an increase in the eddy amplitude.

240 3.3 Regional

241 **Figure 7**



231 **Figure 6.** Hemispherical seasonality of the coherent eddy statistics; a,e) seasonal cycle of the
 232 number of coherent eddies ($cEddy_n$); b,f) seasonal cycle of the mean coherent eddy amplitude
 233 ($cEddy_{amp}$); c,g) seasonal cycle of the warm core coherent eddies amplitude (positive $cEddy_{amp}$);
 234 d,h) seasonal cycle of the cold core coherent eddies amplitude (negative $cEddy_{amp}$). Panels a,b
 235 and c show the northern hemisphere seasonal cycle, while panels d,e, and f correspond to the
 236 southern hemisphere. Dashed lines correspond to the seasonal cycle of the fields and dotted lines
 237 show the seasonal cycle of the wind magnitude smoothed over 120 days (moving average). The
 238 green and magenta stars show the maximum of the seasonal cycle for each field and the wind
 239 magnitude, respectively. The line colors show the year.



254 **Figure 7.** Climatology of the eddy field and coherent eddy field at the Leeuwin Current. a)
 255 Ratio of mean coherent eddy kinetic energy ($\overline{\text{CEKE}}$) versus mean eddy kinetic energy ($\overline{\text{EKE}}$); b)
 256 Thick lines show the running average over 2 years and thin lines show the running average over
 257 90 days of the coherent eddy number sum and the average absolute coherent eddy amplitude; c)
 258 Map of the number of eddies; d) Map of the average absolute coherent eddy amplitude; e) Sea-
 259 sonal cycle of the number of eddies f) Seasonal cycle of the positive coherent eddy amplitude. g)
 260 Seasonal cycle of the negative coherent eddy amplitude.

- 242 • South of the Leeuwin Current there is an important dominance fo the coherent
 243 eddy field, where it explains around 80% of the eddy kinetic energy.
 244 • Although this region does not have a large EKE, we can observe a considerable
 245 amount of eddies across the region, but more importantly the coherent eddy am-
 246 plitude is particularly large in those regions with coherent eddy dominance.
 247 • The solid lines show an decrease in the number of eddies, but an increase in the
 248 eddy amplitude.
 249 • Moreover, the coherent eddy number peaks in August.
 250 • Meanwhile coherent eddies with the positive amplitude have a smaller amplitude
 251 than the negative, furthermore, the positive eddies peak in Jun and show a inter-
 252 annual modulation, while the negative eddies peak in October.
 253 • Research regional dynamics (Add here why we may expect this response.)

261 **Figure 8**

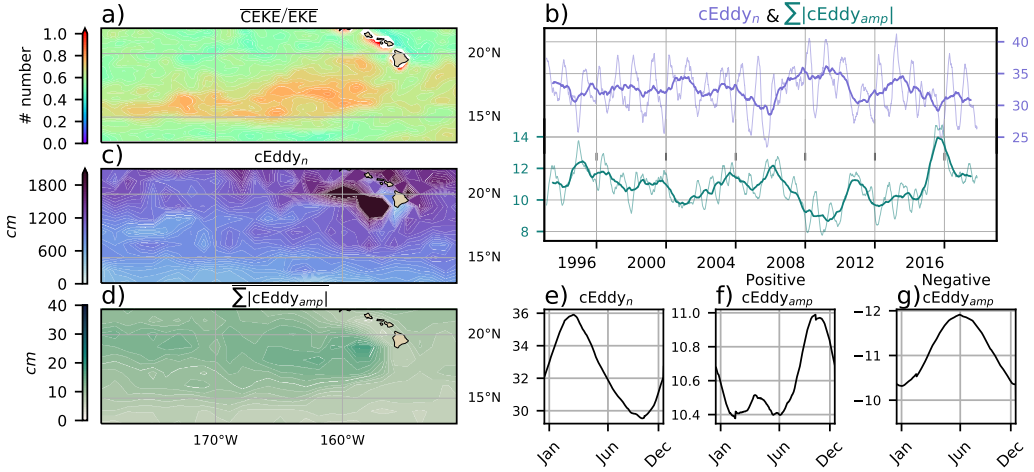


Figure 8. Same as Figure 7 but for the Central North Pacific.

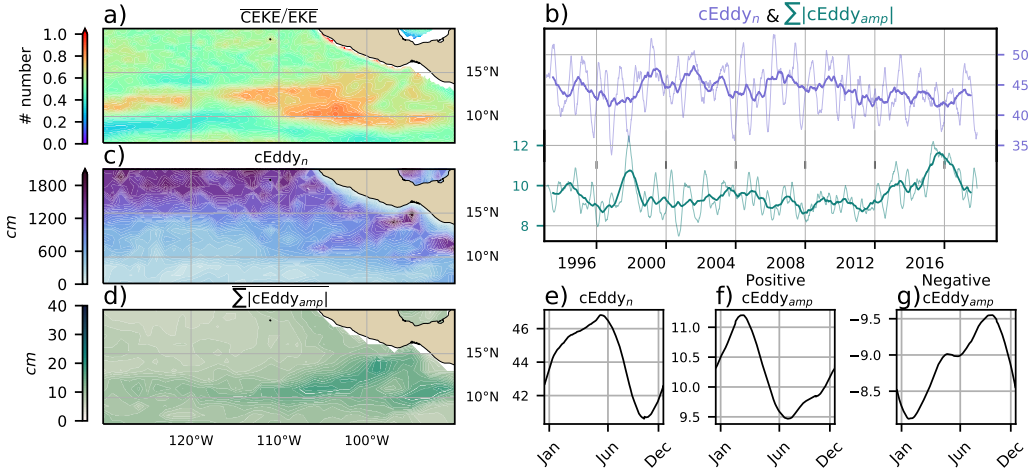
- South west of the Hawai'i there is an important influence of the coherent eddies.
- Although, near we observe a large amount of numbers of eddies in both eddy count form Chelton and JMM, the amplitude is again responsible of the coherent eddy dominance.
- Note the eddy number peaks in March, while the positive eddy amplitude peaks in October, while the negative eddies peak in June.
- Research regional dynamics (Add here why we may expect this response.)

Figure 9

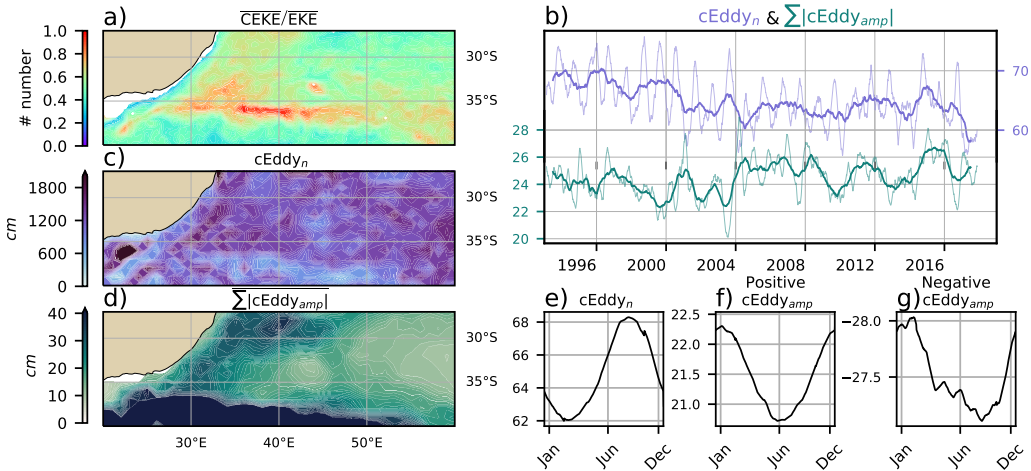
- Here we observe that the number of eddies and eddy amplitude are large in the area where the coherent eddies dominate the eddy field.
- Dynamically, in this region eddies are generated due to Rossby wave propagation along the coast that becomes unstable and sheds eddies at the Tehuantepec Gulf.
- The seasonal cycle shows a peak in Jun, while the positive amplitude is observed in March and the negative amplitude maximum occurs in September.
- Research regional dynamics (Add here why we may expect this response.)

Figure 10

- Described similar to figure 7, 8, and 9



278

Figure 9. Same as Figure 7 but for the East Tropical Pacific.

284

Figure 10. Same as Figure 7 but for the Agulhas Current.

281

282

283

- Note that boundary currents have a consistent seasonal cycle in the positive and negative eddy amplitude.
- As expected, the seasonal cycle is opposite to BC in the northern hemisphere.

285

Figure 11

286

287

288

- Described similar to figure 7, 8, and 9
- Note that boundary currents have a consistent seasonal cycle in the positive and negative eddy amplitude.

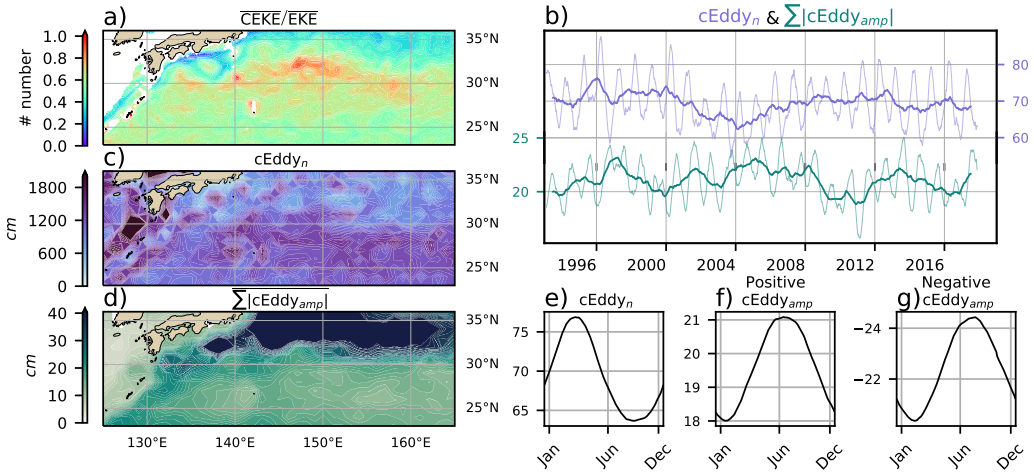


Figure 11. Same as Figure 7 but for the Kuroshio Current.

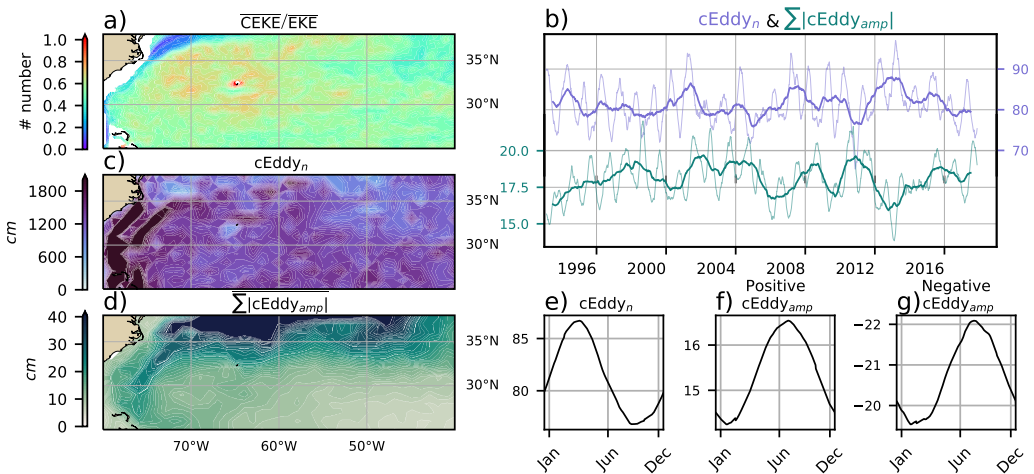
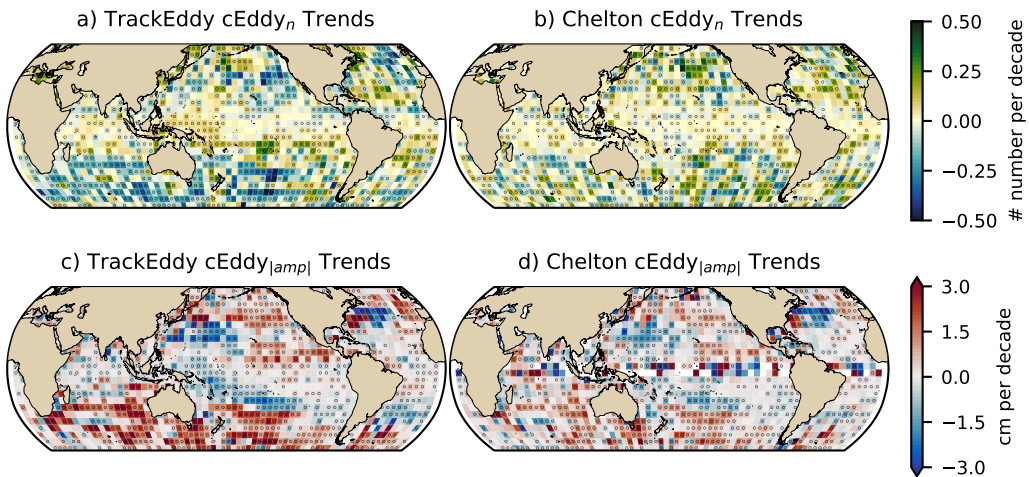


Figure 12. Same as Figure 7 but for the Gulf Stream.

Figure 12

- Described similar to figure 7, 8, and 9
- Note that boundary currents have a consistent seasonal cycle in the positive and negative eddy amplitude.
- Delete Fig 11 or 12, they are really similar. What do you think?



307 **Figure 13.** Trends of coherent eddy statistics. a,b and c Trends of the number of identified
 308 coherent eddies from satellite observations identified using TrackEddy, satellite observations iden-
 309 tified using Chelton's, and state of the art numerical simulation identified using TrackEddy. d,e
 310 and f Trends of the sum of the absolute value of identified coherent eddies amplitude from satel-
 311 lite observations identified using TrackEddy, satellite observations identified using Chelton's, and
 312 state of the art numerical simulation identified using TrackEddy. Gray stippling shows regions
 313 that are statistically significant above the 95% confidence level.

296 4 Trends

297 **Figure 13**

- 298 • The number and amplitude of coherent eddies from two eddy tracking algorithms
 299 show consistent trend patterns.
- 300 • In particular, we observe a decrease in the number of eddies in the southern ocean,
 301 as well as sectors in the North Atlantic and North Pacific.
- 302 • Meanwhile the amplitude seems to be increasing in those same regions.
- 303 • Some of these regions have undergone a readjustment to stronger winds, thus the
 304 observed trends in the eddy amplitude suggests an intensification of the coherent
 305 eddy field to an increase in the forcing.
- 306 • This increase is consistent with Martínez-Moreno et al. (2021)

314 **5 Summary and Conclusions**

315 **Acknowledgments**

316 **References**

- 317 Arbic, B. K., Polzin, K. L., Scott, R. B., Richman, J. G., & Shriver, J. F. (2013).
 On Eddy Viscosity, Energy Cascades, and the Horizontal Resolution of Gridded
 Satellite Altimeter Products*. *Journal of Physical Oceanography*, 43(2), 283–300.
 doi: 10.1175/jpo-d-11-0240.1
- 321 Ashkezari, M. D., Hill, C. N., Follett, C. N., Forget, G., & Follows, M. J. (2016).
 Oceanic eddy detection and lifetime forecast using machine learning methods.
Geophysical Research Letters, 43(23). doi: 10.1002/2016gl071269
- 324 Beron-Vera, F. J., Wang, Y., Olascoaga, M. J., Goni, G. J., & Haller, G. (2013). Ob-
 jective Detection of Oceanic Eddies and the Agulhas Leakage. *Journal of Physical
 Oceanography*, 43(7), 1426–1438. doi: 10.1175/JPO-D-12-0171.1
- 327 Bouali, M., Sato, O. T., & Polito, P. S. (2017). Temporal trends in sea surface tem-
 perature gradients in the South Atlantic Ocean. *Remote Sensing of Environment*,
 194, 100–114. doi: 10.1016/j.rse.2017.03.008
- 330 Callies, J., Flierl, G., Ferrari, R., & Fox-Kemper, B. (2015). The role of mixed-layer
 instabilities in submesoscale turbulence. *Journal of Fluid Mechanics*, 788, 5–41.
 doi: 10.1017/jfm.2015.700
- 333 Cane, M. A., Clement, A. C., Kaplan, A., Kushnir, Y., Pozdnyakov, D., Seager, R.,
 ... Murtugudde, R. (1997). Twentieth-Century Sea Surface Temperature Trends.
Science, 275(5302), 957–960. doi: 10.1126/science.275.5302.957
- 336 Chelton, D. B., Gaube, P., Schlax, M. G., Early, J. J., & Samelson, R. M. (2011).
 The influence of nonlinear mesoscale eddies on near-surface oceanic chlorophyll.
Science, 334(6054), 328-32. doi: 10.1126/science.1208897
- 339 Chelton, D. B., Schlax, M. G., Samelson, R. M., & de Szoeke, R. A. (2007). Global
 observations of large oceanic eddies. *Geophysical Research Letters*, 34(15),
 L15606. doi: 10.1029/2007GL030812
- 342 Cui, W., Wang, W., Zhang, J., & Yang, J. (2020). Identification and census statis-
 tics of multicore eddies based on sea surface height data in global oceans. *Acta
 Oceanologica Sinica*, 39(1), 41–51. doi: 10.1007/s13131-019-1519-y

- 345 Faghmous, J. H., Frenger, I., Yao, Y., Warmka, R., Lindell, A., & Kumar, V. (2015,
346 6). A daily global mesoscale ocean eddy dataset from satellite altimetry. *Scientific
347 Data*, 2, 150028 EP -. doi: 10.1038/sdata.2015.28
- 348 Ferrari, R., & Wunsch, C. (2009). Ocean Circulation Kinetic Energy: Reservoirs,
349 Sources, and Sinks. *Annual Review of Fluid Mechanics*, 41(1), 253–282. doi: 10
350 .1146/annurev.fluid.40.111406.102139
- 351 Frenger, I., Gruber, N., Knutti, R., & Münnich, M. (2013). Imprint of Southern
352 Ocean eddies on winds, clouds and rainfall. *Nature Geoscience*, 6(8), 608 EP -.
353 doi: 10.1038/ngeo1863
- 354 Frenger, I., Münnich, M., Gruber, N., & Knutti, R. (2015). Southern Ocean eddy
355 phenomenology. *Journal of Geophysical Research: Oceans*, 120(11), 7413-7449.
356 doi: 10.1002/2015JC011047
- 357 Fu, L., Chelton, D., Le Traon, P., & Oceanography, M. R. (2010). Eddy dynamics
358 from satellite altimetry. *Oceanography*, 23(4), 14-25. doi: 10.2307/24860859
- 359 Gill, A., Green, J., & Simmons, A. (1974). Energy partition in the large-scale ocean
360 circulation and the production of mid-ocean eddies. *Deep Sea Res Oceanogr Abstr*,
361 21(7), 499-528. doi: 10.1016/0011-7471(74)90010-2
- 362 Hogg, A. M., & Blundell, J. R. (2006). Interdecadal variability of the southern
363 ocean. *Journal of Physical Oceanography*, 36(8), 1626-1645. doi: 10.1175/
364 JPO2934.1
- 365 Hogg, A. M., Meredith, M. P., Chambers, D. P., Abrahamsen, E. P., Hughes,
366 C. W., & Morrison, A. K. (2015). Recent trends in the Southern Ocean
367 eddy field. *Journal of Geophysical Research: Oceans*, 120(1), 257-267. doi:
368 10.1002/2014JC010470
- 369 Hu, S., Sprintall, J., Guan, C., McPhaden, M. J., Wang, F., Hu, D., & Cai,
370 W. (2020, 2). Deep-reaching acceleration of global mean ocean circula-
371 tion over the past two decades. *Science Advances*, 6(6), eaax7727. doi:
372 10.1126/sciadv.aax7727
- 373 Kang, D., & Curchitser, E. N. (2017). On the Evaluation of Seasonal Variability of
374 the Ocean Kinetic Energy. *Geophysical Research Letters*, 47, 1675-1583. doi: 10
375 .1175/JPO-D-17-0063.1
- 376 Li, G., Cheng, L., Zhu, J., Trenberth, K. E., Mann, M. E., & Abraham, J. P. (2020).
377 Increasing ocean stratification over the past half-century. *Nature Climate Change*,

- 378 1–8. doi: 10.1038/s41558-020-00918-2
- 379 Martínez-Moreno, J., Hogg, A. M., England, M., Constantinou, N. C., Kiss, A. E.,
380 & Morrison, A. K. (2021). Global changes in oceanic mesoscale currents over the
381 satellite altimetry record. *Journal of Advances in Modeling Earth Systems*, 0(ja).
382 doi: 10.1029/2019MS001769
- 383 Martínez-Moreno, J., Hogg, A. M., Kiss, A. E., Constantinou, N. C., & Mor-
384 rison, A. K. (2019). Kinetic energy of eddy-like features from sea surface
385 altimetry. *Journal of Advances in Modeling Earth Systems*, 0(ja). doi:
386 10.1029/2019MS001769
- 387 Patel, R. S., Llort, J., Strutton, P. G., Phillips, H. E., Moreau, S., Pardo, P. C.,
388 & Lenton, A. (2020). The Biogeochemical Structure of Southern Ocean
389 Mesoscale Eddies. *Journal of Geophysical Research: Oceans*, 125(8). doi:
390 10.1029/2020jc016115
- 391 Pilo, G. S., Mata, M. M., & Azevedo, J. L. L. (2015). Eddy surface properties and
392 propagation at Southern Hemisphere western boundary current systems. *Ocean
393 Science*, 11(4), 629–641. doi: 10.5194/os-11-629-2015
- 394 Qiu, B. (1999). Seasonal Eddy Field Modulation of the North Pacific Subtropical
395 Countercurrent: TOPEX/Poseidon Observations and Theory. *Journal of Physical
396 Oceanography*, 29(10), 2471–2486. doi: 10.1175/1520-0485(1999)029<2471:sefmot>2
397 .0.co;2
- 398 Qiu, B., & Chen, S. (2004). Seasonal Modulations in the Eddy Field of the South
399 Pacific Ocean. *Journal of Physical Oceanography*, 34(7), 1515–1527. doi: 10.1175/
400 1520-0485(2004)034<1515:smitef>2.0.co;2
- 401 Qiu, B., Chen, S., Klein, P., Sasaki, H., & Sasai, Y. (2014). Seasonal Mesoscale
402 and Submesoscale Eddy Variability along the North Pacific Subtropical Coun-
403 tercurrent. *Journal of Physical Oceanography*, 44(12), 3079–3098. doi:
404 10.1175/jpo-d-14-0071.1
- 405 Ruela, R., Sousa, M. C., deCastro, M., & Dias, J. M. (2020). Global and regional
406 evolution of sea surface temperature under climate change. *Global and Planetary
407 Change*, 190, 103190. doi: 10.1016/j.gloplacha.2020.103190
- 408 Sasaki, H., Klein, P., Qiu, B., & Sasai, Y. (2014). Impact of oceanic-scale inter-
409 actions on the seasonal modulation of ocean dynamics by the atmosphere. *Nature
410 Communications*, 5(1), 5636. doi: 10.1038/ncomms6636

- 411 Schubert, R., Schwarzkopf, F. U., Baschek, B., & Biastoch, A. (2019). Submesoscale
412 Impacts on Mesoscale Agulhas Dynamics. *Journal of Advances in Modeling Earth*
413 *Systems*, 11(8), 2745–2767. doi: 10.1029/2019ms001724
- 414 Siegel, D., Peterson, P., DJ, M., Maritorena, S., & Nelson, N. (2011). Bio-optical
415 footprints created by mesoscale eddies in the Sargasso Sea. *Geophysical Research*
416 *Letters*, 38(13), n/a-n/a. doi: 10.1029/2011GL047660
- 417 Uchida, T., Abernathey, R., & Smith, S. (2017). Seasonality of eddy kinetic energy
418 in an eddy permitting global climate model. *Ocean Modelling*, 118, 41-58. doi: 10
419 .1016/j.ocemod.2017.08.006
- 420 Wunsch, C. (2020). Is The Ocean Speeding Up? Ocean Surface Energy Trends.
421 *Journal of Physical Oceanography*, 50(11), 1–45. doi: 10.1175/jpo-d-20-0082.1
- 422 Wunsch, C., & Ferrari, R. (2004). VERTICAL MIXING, ENERGY, AND THE
423 GENERAL CIRCULATION OF THE OCEANS. *Annual Review of Fluid Me-*
424 *chanics*, 36(1), 281–314. doi: 10.1146/annurev.fluid.36.050802.122121
- 425 Wyrtki, K., Magaard, L., & Hager, J. (1976). Eddy energy in the oceans. *Journal of*
426 *Geophysical Research*, 81(15), 2641-2646. doi: 10.1029/JC081i015p02641